Rapid nongenomic estrogen signaling controls alcohol drinking behavior

Zallar, L.J.[1], Rivera-Irizarry, J.K.[2], Hamor, P.U.[3], Pigulevskiy[1], I., Liu, D.[3], Welday, J.P.[2], Rico Rozo, A.S.[3], Bender, R.[3], Asfouri, J.[3], Levine, O.B.[2], Skelly, M.J.[3,a], Hadley, C.K.[5], Fecteau, K.M.[4], Mehanna, H.[3], Nelson, S.[3], Miller, J.[3], Ghazal, P.[3,b], Bellotti, P.[3], Singh, A.[2], Hollmer, L.V.[1] Erikson, D.W.[4], Geri, J.[3], Pleil, K.E.[1,2,3^]

[1]Pharmacology Graduate Program, Weill Cornell Graduate School of Medical Sciences, Weill Cornell Medicine, Cornell University, New York, NY, USA
[2]Neuroscience Graduate Program, Weill Cornell Graduate School of Medical Sciences, Weill Cornell Medicine, Cornell University, New York, NY, USA
[3]Department of Pharmacology, Weill Cornell Medicine, Cornell University, New York, NY, USA
[4]Endocrine Technologies Core, Oregon National Primate Research Center, Beaverton, OR, USA
[5]Weill Cornell/Rockefeller/Sloan Kettering Tri-institutional MD-PhD Program, New York, NY 10065, USA.
[a]Current affiliation: Psychology Department, Iona University, New Rochelle, NY, USA
[b]Current affiliation: Department of Biosciences, COMSATS University Islamabad (CUI), Islamabad, Pakistan
^correspondence can be directed to krp2013@med.cornell.edu

Abstract

The sex steroid hormone estrogen is a key modulator of numerous physiological processes and adaptive behaviors, but it may also be co-opted to drive maladaptive behaviors. While many behavioral roles for estrogen signaling have been shown to occur through canonical genomic signaling mechanisms via nuclear receptors, estrogen can also act in a neurotransmitter-like fashion at membrane-associated estrogen receptors to rapidly regulate neuronal function. Early alcohol drinking confers greater risk for alcohol use disorder in women than men, and binge alcohol drinking is correlated with high circulating estrogen but a causal role for estrogen in alcohol drinking has not been established. Here, we demonstrate that gonadally intact female mice consume more alcohol and display an anxiolytic phenotype when they have elevated levels of ovarian-derived estrogen across the estrous cycle. We found that rapid, nongenomic estrogen signaling at membrane-associated estrogen receptor alpha in the bed nucleus of the stria terminalis (BNST) is necessary and sufficient for the pro-alcohol drinking effects of ovarian estrogen signaling, regardless of the transcriptional program of a high ovarian estrogen state. We further show that a population of corticotropin-releasing factor (CRF) BNST neurons ($BNST^{CRF}$) is a critical mediator of these effects, as high estrogen rapidly enhances synaptic excitation of $BNST^{CRF}$ neurons and promotes their role in driving binge alcohol drinking. These findings show a causal role for endogenous, ovarian-derived estrogen in hormonal modulation of risky alcohol consumption and provide the first demonstration of a purely rapid, nongenomic signaling mechanism of ovarian estrogen in the brain controlling behavior in gonadally intact females.

Introduction

Sex is a major regulator of behavior across species, but the numerous underlying neurobiological mechanisms that mediate these differences are not fully characterized[1]. One key neuromodulator of behavior is the sex steroid hormone estrogen (17β-estradiol; E2) which is produced in high volumes in the ovaries of females during the menstrual cycle in humans and estrous cycle in rodents[2]. E2 signaling is critical for the maintenance of numerous adaptive behaviors in both sexes, such as reproduction[3], learning and memory[4,5], and emotional behaviors[6], but it may also support maladaptive behaviors related to neuropsychiatric diseases[7-9]. E2 has been classically described to affect behavior through its engagement with nuclear estrogen receptors (ERs) to produce broad transcriptional changes via genomic mechanisms[10]. However, it can also act at membrane-associated ERs in the brain to rapidly modulate synaptic transmission and intrinsic excitability in brain regions including the hippocampus, hypothalamus, striatum, nucleus accumbens, and amygdala[5,11-17]. Pioneering work has established that rapid E2 signaling plays a critical role in the mediation of behavior, as acute administration of E2 or ER modulators can modulate behaviors including aggression[18,19] and reproductive/sexual behavior[20] in gonadectomized male rodents, as well as learning and memory[21,22] and psychostimulant self-administration and hyperlocomotion in ovariectomized female rodents[23-25], within an hour of administration. However, the role of rapid E2 signaling in intact rodents is relatively unknown, with the exception of a report showing that acute pharmacological inhibition of E2 synthesis rapidly inhibits male sexual behavior[26]. Studies tying rapid E2 signaling mechanisms to behavior modulation in intact subjects has been primarily studied in birds, in which E2 produced locally at discrete synapses via local aromatization of testosterone rapidly regulates neuronal function to mediate birdsong and reproductive behaviors[27-31]. Thus, the behavioral roles for rapid signaling of ovarian-derived E2 in gonadally intact females and the mechanisms by which these effects occur have yet to be described.

There is significant evidence that E2 may be a key neuromodulator driving alcohol and drug-related behaviors[8,32-34], including excessive alcohol consumption[9,35,36], which is a primary risk factor for numerous disease states including alcohol use disorder (AUD) and anxiety disorders[37-41]. Women exhibit an accelerated onset of, and a higher probability for developing, AUD with the same history of alcohol use as their male counterparts in a phenomenon known as the telescoping effect; further, binge-like patterns of alcohol consumption are increasingly prevalent[39,42-44]. Both binge alcohol drinking and related diseases emerge in women during puberty when ovarian-derived and related hormones begin to fluctuate across the menstrual cycle, and decades of research have found positive associations between circulating concentration of ovarian E2 across the menstrual cycle and alcohol drinking behavior[45-48]. It is well-established in preclinical rodent models that females consume more alcohol than their male counterparts[49-53], and ovarian hormones likely contribute to this phenomenon. Both removal of the ovaries and degradation of estrogen receptors (ERs) in the brain reduce alcohol drinking[9,35], and chronic E2 administration in ovariectomized females can restore high alcohol drinking in some cases[9,54-57]. However, a specific role for fluctuating E2 across the estrous cycle in intact female alcohol drinking behavior has not been established, nor mechanistic insight into its role.

Here, we show that the bed nucleus of the stria terminalis (BNST), one of the most sexually dimorphic brain regions that robustly expresses ERs[58,59], is a critical site for the effects of ovarian E2 signaling in driving alcohol drinking, but not avoidance behavior, in female mice. We show that these pro-drinking effects occur via rapid nongenomic signaling at membrane-associated ERα. Further, we find that BNST neurons that synthesize and release corticotropin releasing factor (CRF), a stress neuropeptide known to play a role in alcohol and anxiety-related behaviors[60-63] across mammalian species, is critical to this behavioral role of E2 through rapid E2-mediated synaptic excitation and enhancement of activity during motivated alcohol drinking behavior.

Results

E2 status across the estrous cycle dictates binge alcohol drinking and avoidance behavior

Prior studies have been unable to show dynamic modulation of alcohol drinking across the 4-5 day estrous cycle or a causal role for E2 in motivated alcohol drinking in gonadally intact female rodents, perhaps due to practical considerations including behavioral testing in the dark phase of the light/dark cycle, potential disruption to estrous cyclicity by daily monitoring techniques, and the relatively transient peak of E2 in rodents. Here, we validated and employed a minimally-invasive strategy to chronically monitor daily estrous cycle phase in intact female mice in close temporal proximity to behavioral testing during the dark phase of the light/dark

cycle (**Fig. 1a–c; Extended Data Fig. 1a-c**). Two hrs into the dark cycle each day, vaginal epithelial cells were collected via saline lavage and used to determine estrous cycle phase (**Fig. 1a**). Mice categorized as being in proestrus had higher ovarian expression of aromatase, the rate-limiting enzyme required for E2 synthesis (**Fig. 1b**) and higher blood plasma E2 concentrations (**Fig. 1c**) than females in metestrus, confirming that mice categorized as being in proestrus using vaginal lavage-derived cytology were in a high ovarian E2 state (high E2) compared to those mice categorized as being in a low E2 state. Measures including estrous cycle length and the number of days in proestrus per estrous cycle were similar when lavage was performed in the light phase of the light cycle, and normal estrous cyclicity remained consistent across many weeks of daily monitoring (**Extended Data Fig. 1a-c**). Therefore, we were able to use this vaginal cytology tracking strategy as an accurate, minimally-invasive proxy measure of real-time E2 status in intact female mice during behavioral testing in the dark phase without disrupting their natural estrous cyclicity and hormonal milieu.

We first employed this strategy to assess the effects of high E2 status during the estrous cycle on binge alcohol drinking using the standard drinking in the dark (DID) paradigm in which mice receive limited access (2-4 hrs/day, 4 consecutive days per cycle) to 20% EtOH instead of their home cage water bottle (**Fig. 1d**). Across weekly cycles of alcohol DID, individual females consumed more alcohol when they were in a high E2 state in proestrus compared to when they were in other estrous cycle phases, with alcohol consumption during low E2 days increasing until it converged with the high E2 level by cycle six (**Fig. 1e**), demonstrating that individual females consume more alcohol when in a high ovarian E2 state than low ovarian E2 state. There was no significant difference in alcohol consumption between low E2 females and males, suggesting that ovarian E2 contributes to the higher consumption in females than males that we and others have previously reported[49,64,65]. Intriguingly, we found that when females were specifically given their first access to alcohol in a high ovarian E2 state in proestrus, they consumed more alcohol than conspecifics given first access in a low E2 state during metestrus (**Fig. 1f**), suggesting that prior experience with alcohol was not required for the pro-drinking effect of E2 status on binge drinking behavior. Further, there was no correlation between the cumulative number of alcohol drinking sessions in a high E2 state and alcohol consumption in subsequent low E2 sessions within individual mice across the six alcohol DID cycles (**Extended Data Fig. 1d**), suggesting that the acute stimulatory effect of high E2 state on alcohol drinking was not directly related to the gradual escalation in low E2 alcohol consumption across DID cycles. In contrast to alcohol intake, ovarian E2 did not affect consumption of 1% sucrose in a matched DID paradigm (sucrose-DID; **Fig. 1g, h**). Males and females in high and low E2 states showed similar sucrose intake across cycles of sucrose-DID (**Fig. 1g**) and during their first access to sucrose (**Fig. 1h**), suggesting the effects of ovarian E2 status on alcohol drinking are not due to general increased liquid consumption or appetitive regulation.

Alcohol drinking phenotypes are often associated with dysregulation of anxiety behavior[66]. While there is evidence that both are sensitive to ovarian E2 in humans and rodents[36,47,67,68], the association between E2 signaling and avoidance is ambiguous in the literature, with some finding estrous-dependent anxiety-like behavior[69] and others reporting no effect of chronic E2 on anxiety-like behavior in gonadally intact females[70]. Therefore, to further elucidate this relationship, we examined whether ovarian E2 could also dynamically regulate avoidance behavior in individual mice. Across a battery of avoidance behavior assays, females in a high E2 state displayed an anxiolytic phenotype compared to conspecifics in a low E2 state and males, with greater % time spent and distance in the center of the open field (OF), light side of the light/dark box (LDB), and open arms of the elevated plus maze (EPM), without any alteration in their overall locomotor behavior (**Fig. 1i-m; Extended Data Fig. 1e,f**). Individual females' behavior varied according to their estrous cycle stage across the assays, suggesting that ovarian E2 is a critical real-time regulator of avoidance behavior at the individual level, even when mice have had prior experiences in experimentally-induced anxiogenic contexts.

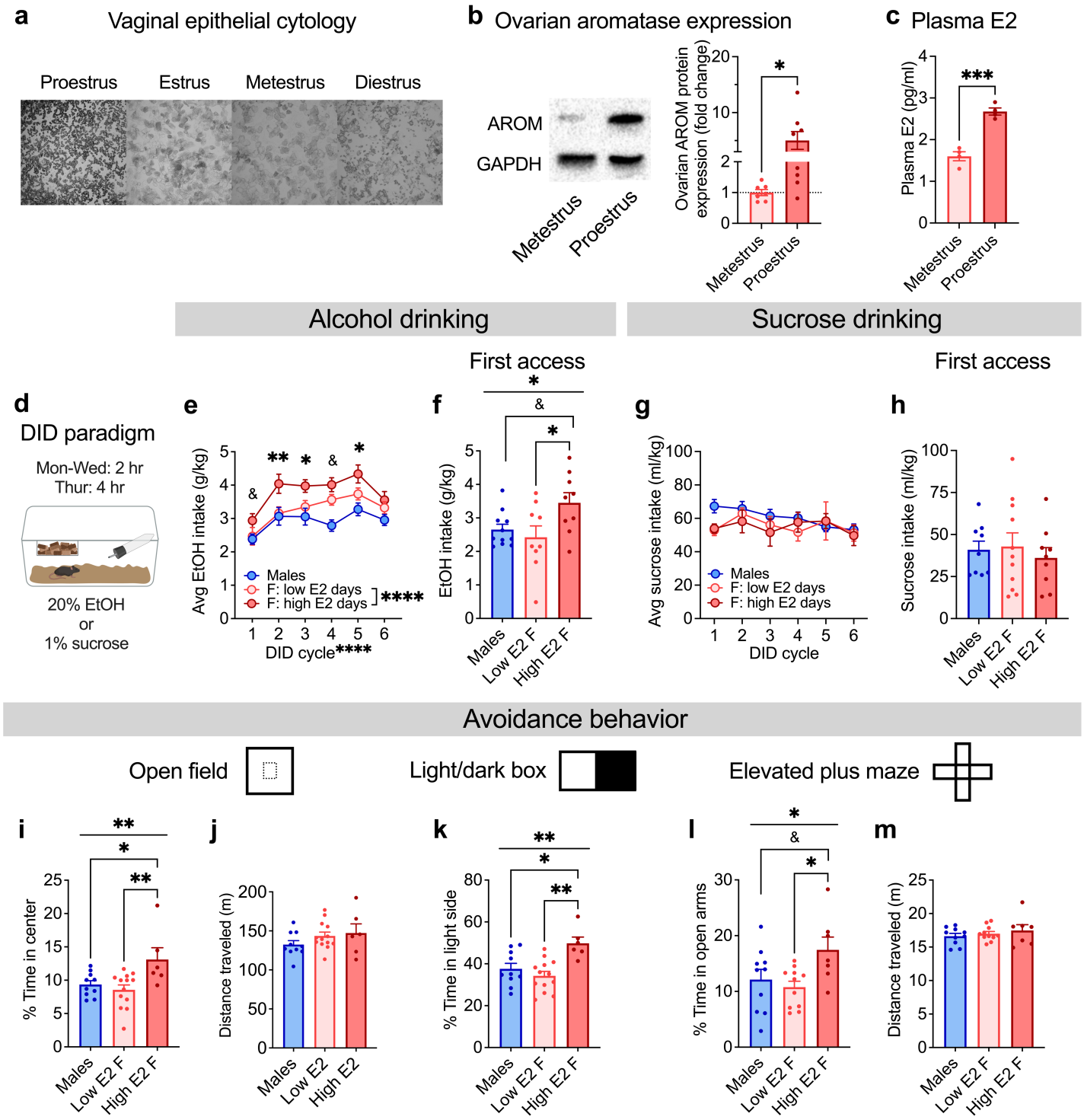

Figure 1: Binge alcohol drinking and avoidance behavior fluctuate with E2 status across the estrous cycle in gonadally-intact female mice. a-c) Minimally-invasive method for monitoring E2 status across the estrous cycle in gonadally-intact C57BL/6J mice. **a)** Representative images of vaginal epithelial cells in each estrous cycle phase in the female mouse. **b)** Aromatase protein expression normalized to glyceraldehyde 3-phosphate dehydrogenase (GAPDH) was higher in the ovaries of female mice categorized as being in proestrus compared to mice categorized as being in metestrus. **c)** Plasma E2 concentrations were higher in proestrus compared to metestrus female mice, where each data point represents a pooled sample from five mice. **d-h)** Females consume more alcohol but not sucrose when they are in a high ovarian E2 state than low ovarian E2 state and than males. **d)** Schematic of the Drinking in the Dark (DID) binge consumption paradigm used in intact mice. **e)** High E2 status promotes average 2-hr consumption of 20% alcohol across cycles of alcohol DID in males and females. Within each DID cycle, individual females' average consumption on day(s) in proestrus when ovarian E2 was high vs. their days in other estrous cycle phases when ovarian E2 was low is included for each cycle in which mice had proestrus drinking day(s). **f)** Females given access to alcohol for the first time in a high E2 state (proestrus) displayed greater binge drinking than those given first access in a low E2 state (metestrus) and males. **g)**

Estrous cycle stage dose not modulate average 2-hr consumption of 1% sucrose across DID cycles (measured as for alcohol in **e**). **h)** Females given access sucrose for the first time in a high E2 state display similar binge drinking to those given first access in a low E2 state and males. **i**–**m)** Females in a higher ovarian E2 state display reduced avoidance behavior compared to low E2 females and males. **i)** % Time spent in the center of the open field test (OF) in males and females in proestrus (high E2) or other estrous cycle stages (low E2). **j)** Distance traveled in the OF. **k)** % Time spent on the light side of the light/dark box (LDB) in males, low E2 F, and high E2 F. **l)** % Time spent in open arms of the elevated plus maze (EPM) in males, low E2 F, and high E2 F. **m)** Distance traveled in the EPM. *P < 0.05, **P < 0.01, ***P < 0.001, ****P < 0.0001, $^{\&}$P < 0.10 for unpaired t-tests, mixed effects analysis main effects, one way ANOVA main effects of group, and post hoc t-tests paired t-tests with H-S corrections between high and low E2 days in e and post hoc unpaired t-tests with H-S corrections for other panels, as indicated. All schematics created with biorender.com.

Ovarian E2 enhances synaptic excitation of BNST^{CRF} neurons and their pro-alcohol drinking role

Data from human patients with alcohol use disorder and anxiety disorders show that the BNST is an important hub of neurocircuitry that is altered in these disease states[71,72], and the BNST is critical in the regulation of binge alcohol drinking and avoidance behavior in rodents[49,73]. We and others have shown that a major subpopulation of BNST neurons that synthesize and release the stress neuropeptide corticotropin-releasing factor (CRF) is especially important for role of the BNST in alcohol drinking in both sexes and avoidance behavior in males (females not examined) [49]. We recently reported that BNST^{CRF} neurons in females display greater basal excitability and glutamatergic synaptic excitation than in males, which may be related to their higher alcohol drinking[49]. Here, using a multiplexed chemogenetic manipulation approach (**Fig. 2a-d; Extended Data Fig. 2**), we found that the activity of BNST^{CRF} neurons is required for binge alcohol drinking but does not modulate avoidance behavior in females, as chemogenetic inhibition suppressed alcohol consumption (**Fig. 2c**) but did not alter avoidance behavior on the EPM (**Fig. 2d**).

We then examined whether ovarian E2 status regulates BNST^{CRF} neuron function and activation during behavior utilizing converging *ex vivo* and *in vivo* approaches. During slice electrophysiology recordings (**Fig. 2e-m**), we found that BNST^{CRF} neurons from females in a high ovarian E2 state had a higher frequency, but not amplitude, of spontaneous excitatory postsynaptic currents (sEPSCs) than those from females in a low ovarian E2 state (**Fig. 2g,h**), leading to greater excitatory synaptic drive (**Fig. 2i**). BNST^{CRF} neurons from high E2 females also displayed higher frequency, but not amplitude, of spontaneous inhibitory postsynaptic currents (sIPSCs; **Fig. 2k,l**) but this was insufficient to enhance inhibitory synaptic drive (**Fig. 2m**). Using *in vivo* fiber photometry monitoring of the calcium biosensor GCaMP6s in BNST^{CRF} neurons as a proxy for neuronal activity during a modified alcohol DID task in which mice received water access before and after alcohol each day (**Fig. 2n-u; Extended Data Fig. 3**), mice displayed robust motivated drinking behavior specifically during the first 30 min of alcohol access (**Fig. 2q,r**). In particular, there was an increase in motivated drinking bouts between water access and the first 30 min of alcohol access, which was more robust when females were in a high E2 than low E2 state (**Fig. 2r**; **Extended Data Fig. 3d,e**). In contrast, there was no change in the number of drinking bouts between the last 30 min of alcohol access and second water access (**Extended Data Fig. 3f**) and total time spent drinking as measured by the total number of licks across the session was similar between high and low E2 state drinking days (**Extended Data Fig. 3c**), suggesting that the effect of high E2 on motivated drinking was specific to the early alcohol access period. Normalized GCaMP signal in BNST^{CRF} neurons z-scored to the entire drinking session was also selectively increased during the first 30 min of alcohol access and to a higher degree on days when mice were in high ovarian E2 state than low ovarian E2 state (**Fig. 2p,s,t**). Further, the GCaMP signal was elevated during alcohol drinking bouts but not water drinking bouts on both high E2 and low E2 drinking days (**Extended Data Fig. 3h,i**) and the time spent drinking alcohol was positively correlated with GCaMP signal during the first 30 min of alcohol access (**Fig. 2u**). In contrast, fiber photometry recordings of BNST^{CRF} GCaMP during EPM (**Extended Data Fig. 3j-l**) and OF (**Extended Data Fig. 3m-o**) showed that while GCaMP activity in BNST^{CRF} neurons was highest in the anxiogenic compartments of the mazes (open arms of EPM and center of OF), it was similar between low E2 and high E2 conditions. Altogether, these results suggest that high ovarian E2 state-dependent excitation of BNST^{CRF} neurons drives the pro-drinking, but not anxiolytic, phenotype observed in proestrus.

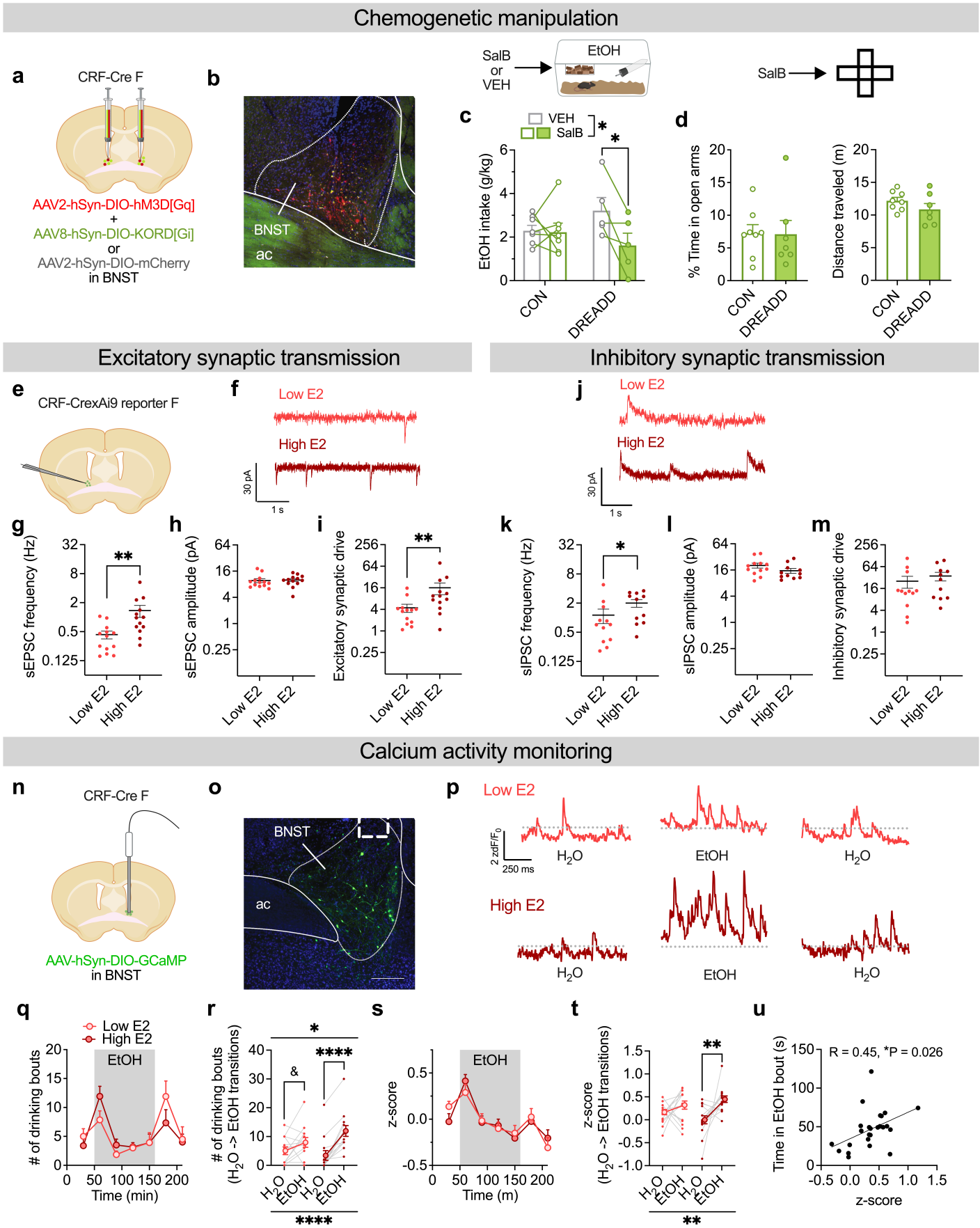

Fig. 2: Ovarian E2 state modulates the synaptic excitation of BNST^{CRF} neurons and their activity during motivated binge drinking. a-d) Chemogenetic manipulation of BNST^{CRF} neurons during binge alcohol drinking and avoidance behaviors. **a-b)** Schematic (**a**) and representative image (**b**) for viral strategy to bidirectionally manipulate BNST^{CRF} neurons using a multiplexed Gi/Gq DREADD approach. **c-d)** Activation of the Gi-coupled KOR DREADD via systemic

injection of Salvinorin B (SalB; 10 mg/kg) suppressed binge alcohol consumption compared to vehicle (VEH) injected controls (**c**) but did not affect the % time in open arms or distance traveled in the EPM (**d**). **e-m)** Spontaneous synaptic transmission in $BNST^{CRF}$ neurons as measured in slice electrophysiology recordings from intact CRF-CrexAi9 reporter females in low vs. high ovarian E2 states, with schematic in **e**. **f)** Representative traces of spontaneous excitatory postsynaptic currents (sEPSCs). **g)** The frequency of sEPSCs was higher in $BNST^{CRF}$ neurons from high ovarian E2 females than those from low E2 females. **h)** sEPSC amplitude was unaffected by ovarian E2 status. **i)** The excitatory synaptic drive onto $BNST^{CRF}$ neurons (frequency x amplitude) was greater in high vs. low ovarian E2 females. **j)** Representative traces of spontaneous inhibitory postsynaptic currents (sIPSCs). **k-m)** sIPSC frequency in $BNST^{CRF}$ neurons was greater in high vs. low ovarian E2 status females (**k**), but amplitude (**l**) and synaptic drive (**m**) did not differ. **n-u)** Fiber photometry recordings of GCamP6s in $BNST^{CRF}$ neurons during behavior, with schematic of unilateral viral injection and optical fiber cannula placement in **n** and representative image of GCaMP expression and fiber placement in **o**. **p)** Representative GCaMP traces from one mouse during modified alcohol DID drinking sessions in which water was provided before and after 2-hr alcohol access, with a day that the mouse was in a low E2 state on the top row and a day the same mouse was in high E2 state on the bottom row. **q)** Time course showing drinking bouts across the water and alcohol epochs in 30 min bins, with gray shading representing the alcohol-ON epoch. **r)** The number of drinking bouts increased during the first 30 min of alcohol access compared to the preceding 30 min of water access more robustly when females were in a high E2 state than when they were in a low E2 state. **s)** Time course of GCaMP signal normalized across the entire session of DID, shown in 30 min bins as for drinking bouts in **q**. **t)** The GCaMP signal was elevated in high E2, but not low E2, mice during the first 30 min of alcohol access compared to the preceding 30 min of water access. **u)** During the first 30 min of alcohol access, there was a positive correlation between GCaMP signal and the time spent in motivated drinking bouts for days with ≥ 2 bouts. *$P < 0.05$, **$P < 0.01$, ****$P < 0.0001$, $^{\&}P < 0.10$ for unpaired t-tests, 2xANOVA main effects and interactions and their *post hoc* paired t-tests with H-S corrections, and Pearson's correlation as indicated. All schematics created with biorender.com.

Rapid nongenomic E2 signaling in the BNST promotes binge alcohol drinking and synaptic excitation of $BNST^{CRF}$ neurons

We next assessed the timescale on which ovarian E2 status can regulate binge alcohol drinking and avoidance behaviors. We found that systemic administration of the aromatase inhibitor letrozole (LET) to acutely block E2 synthesis (and thus acutely reduce E2 bioavailability) dose-dependently suppressed binge alcohol consumption in females in a high ovarian E2 state (**Fig. 3b**) but not in a low ovarian E2 state (**Extended Data Fig. 4a**). Acute LET had no effect on binge sucrose consumption in either high or low ovarian E2 females (**Extended Data Fig. 4c,d**), suggesting that ovarian E2's role in promoting alcohol drinking is not due to modulation of general appetitive behavior or reward sensitivity. In addition, acute LET administration did not attenuate high E2-mediated anxiolysis in the EPM (**Fig. 3c,d**). Together, these results demonstrate that acute E2 bioavailability and signaling are necessary for the pro-alcohol drinking, but not anxiolytic, effects of high ovarian E2 status.

As E2 availability in real time was required for the pro-alcohol drinking effects of ovarian E2, we next sought to understand whether the BNST is a critical site for the behavioral effects of rapid E2 signaling via nongenomic signaling at the cell membrane (**Fig. 3e-h**). We found that acute intra-BNST infusion of E2 (20 pg/side) in low E2 status females 10 min prior to behavioral testing rapidly enhanced binge alcohol consumption measured at 1- and 2-hrs (**Fig. 3f**) We further found that intra-BNST infusion of a purified BSA-conjugated E2, which cannot cross the cell membrane and thus can only signal at membrane-associated receptors (mem-E2), and which has previously been found to mediate memory consolidation in ovariectomized female mice[74], also rapidly increased binge alcohol drinking in low E2 females (**Fig. 3g**). In contrast, acute intra-BNST infusion of E2 had no effect on avoidance behavior or locomotion on the EPM (**Fig. 3h**). These results suggest that the BNST is a site for the rapid E2 signaling effects of high ovarian E2 status driving binge alcohol drinking behavior through nongenomic E2 signaling at membrane-associated ERs; further, they suggest that the E2-induced transcriptional program of high ovarian E2 status is not required for these pro-drinking effects but may be required for the anxiolytic effects of high ovarian E2 status.

Because $BNST^{CRF}$ neuron activation and acute E2 signaling in the BNST both rapidly enhanced binge alcohol drinking, we tested whether E2 rapidly promotes synaptic excitation of $BNST^{CRF}$ neurons in slice electrophysiology recordings (**Fig. 3i-l**). We found that bath application of E2 across a range of doses (1 nM-1 μM) robustly increased the frequency of sEPSCs in a large subset (45%) of $BNST^{CRF}$ neurons in low ovarian E2 females (**Fig. 3j; Extended Data Fig. 5a,b**); heterogeneity in response to E2 application has been similarly described previously[75,76]. sEPSC frequency was modulated by rapid E2 signaling to a greater degree than sEPSC amplitude, and E2 modulation of frequency and amplitude were unrelated to each other or their

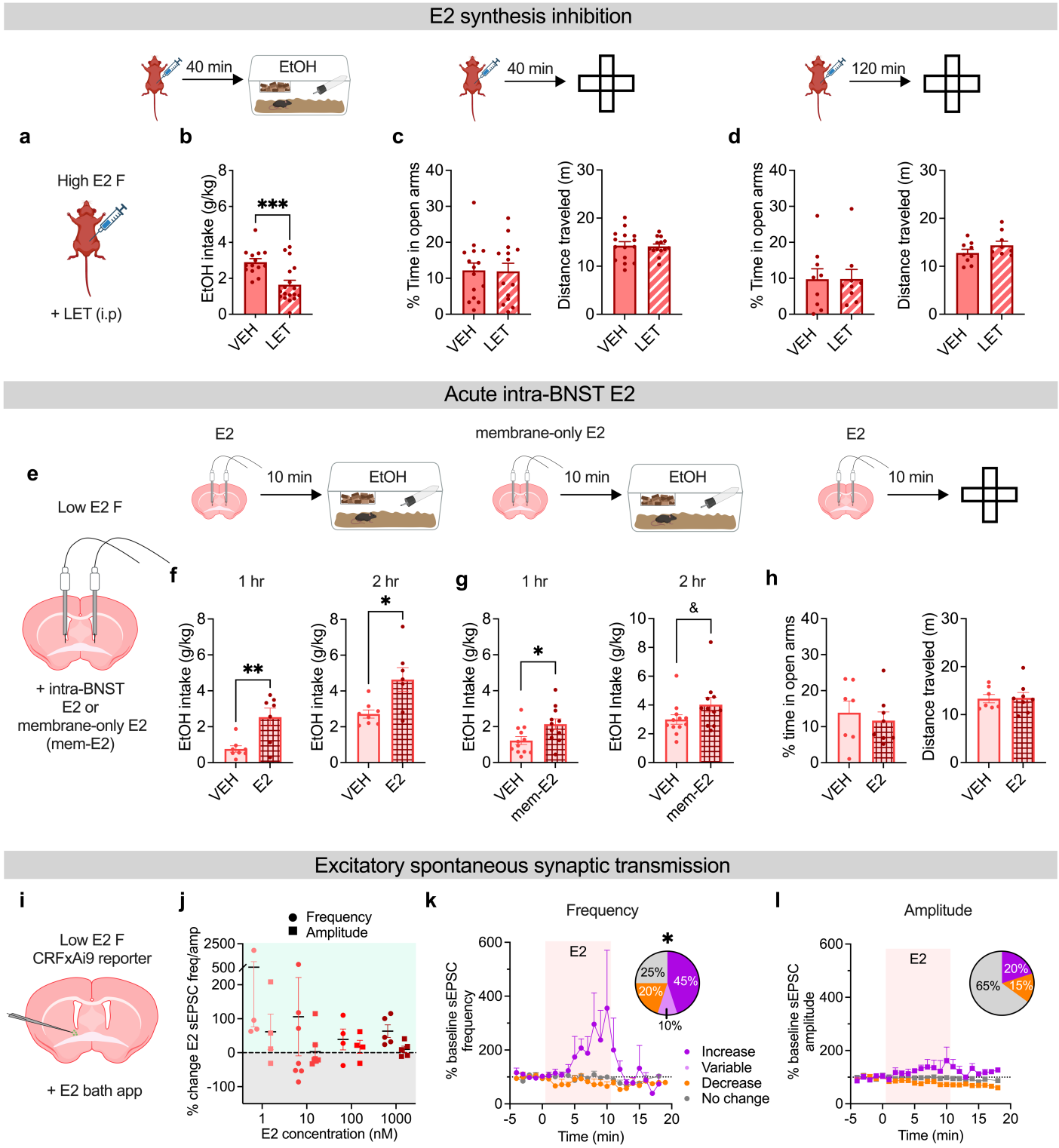

Figure 3: Rapid E2 signaling in the BNST recapitulates the pro-drinking but not anxiolytic effects of ovarian E2 and modulates BNST^{CRF} neurons. a–d) Effects of acute systemic E2 synthesis inhibition on behavior in high ovarian E2 mice using systemic administration of the aromatase activity inhibitor letrozole (LET, 10 mg/kg, i.p.), as depicted in **a**. **b)** Acute LET administration 40 min prior to alcohol access suppressed binge alcohol consumption in high E2 females. **c)** Acute LET administration in high E2 females 1 hr prior to EPM did not alter the % time spent in the open arms. **d)** Acute LET administration in high E2 females 2 hrs prior to EPM did not alter the % time spent in the open arms. **e–h)** Effects of acute intra-BNST infusion of free E2 (20 pg in 200 nl/side) or BSA-conjugated, membrane-impermeable E2 (mem-E2, 55 pg in 200 nl/side) or vehicle controls (VEH) in low ovarian E2 females on behavior, as depicted in **e**. **f)** Intra-BNST E2 delivered 10 min prior to alcohol access promoted binge alcohol consumption in low E2 females at the 1-hr and 2-hr time points. **g)** Intra-BNST E2-BSA, which cannot cross the cell membrane, delivered 10 min prior to alcohol access increased binge alcohol drinking in low ovarian E2 females at the 1-hr timepoint with a trend at the 2-hr timepoint. **h)** Intra-BNST E2

delivered 10 min prior to testing on the elevated plus maze (EPM) had no effect on % time spent in the open arms. **i-l)** Effects of acute bath application of E2 on excitatory synaptic transmission in $BNST^{CRF}$ neurons during whole-cell slice electrophysiology recordings in low ovarian E2 female CRF-CrexAi9 reporter mice, as depicted in **i**. **j)** Spontaneous excitatory postsynaptic currents (sEPSCs) maximum delta from % baseline during E2 wash on. **k)** Time course of $BNST^{CRF}$ neurons that displayed an increase, decrease, or no change in spontaneous excitatory postsynaptic current (sEPSC) frequency % change from baseline during the 10-min application period and proportion of responding $BNST^{CRF}$ neuron categories during E2 wash on (pie chart). **l**) Time course of $BNST^{CRF}$ neurons that displayed an increase, decrease, or no change in sEPSC amplitude % change from baseline during the 10-min application period and responding $BNST^{CRF}$ neuron categories during E2 wash on (pie chart). *P < 0.05, **P < 0.01, ***P < 0.001, unpaired t-tests between VEH vs. LET treatment and VEH vs E2/mem-E2 treatment; Fisher's exact test frequency vs amplitude; post hoc t-tests with H-S corrections as indicated. &P < 0.10 for t-tests. All schematics created with biorender.com.

baseline values (**Fig. 3k,l; Extended Data Fig. 5c,d**). The enhancement of sEPSC frequency but not amplitude by bath-applied E2 (**Fig. 3k,l)** recapitulated the effects observed in high E2 status females (**Fig. 2. g,h**), peaking at an average of 355% of baseline during the 10 min E2 application period and returning to baseline during washout (**Fig. 3l**). These data suggest that E2 signals via a rapid nongenomic mechanism to promote synaptic excitation of $BNST^{CRF}$ neurons, and this mechanism may contribute to the pro-alcohol drinking role of rapid E2 signaling in the BNST.

ERα mediates the effects of rapid E2 signaling in the BNST

To investigate the receptor(s) mediating E2 drive of alcohol drinking, we examined the expression of ERs in BNST circuits. Analysis of single nucleus RNA sequencing (snRNA-seq) dataset (GEO: GSE126836)[77] showed
that ERα (*Esr1*) was robustly expressed in the BNST (29.3%), while ERβ (*Esr2*) was sparsely expressed (6.7%; **Fig. 4a-c**), and the membrane-only receptor GPER (*Gper1*) was nearly undetected (0.3%; not shown). ERα was enriched in subpopulations of BNST cells that modulate glutamatergic transmission at $BNST^{CRF}$ synapses, including CRF neurons themselves, VGLUT2+ (*Slc17a6*) glutamatergic BNST neurons, and astrocytes (*Gfap)* that regulate synaptic glutamate levels (**Fig. 4a-c, Extended Data. Fig. 6a-d)**. We confirmed ERα and ERβ expression profiles in the BNST using high-sensitivity RNAscope fluorescence *in situ* hybridization (FISH). ERα was robustly expressed and ERβ sparsely expressed in CRF+ neurons (**Fig. 4d**) and VGLUT2+ neurons (**Fig. 4e**) in the BNST. We then probed the roles of ERα and ERβ in the BNST on the rapid behavioral effects of E2 using intra-BNST administration of the ERα antagonist methyl-piperidino-pyrazole (MPP; 10 μM) or ERβ antagonist 4-[2-phenyl-5,7-bis(trifluoromethyl)pyrazolo[1,5-a]pyrimidin-3-yl]phenol (PPTHP; 10 μM) or their control vehicles just before behavioral testing (**Fig. 4f**). We found that acutely blocking ERα, but not ERβ, signaling in the BNST abolished the pro-alcohol drinking effects of high E2 status (**Fig. 4g**), while neither affected avoidance behavior (**Fig. 4h,i**). Altogether, our results suggest that rapid E2 signaling at membrane-bound ERα mediates the pro-alcohol drinking effects of high ovarian E2 status in intact female mice. In contrast, the transcriptional program of high ovarian E2 status may be necessary for its anxiolytic effects.

Discussion

Here, we describe a critical role for rapid E2 signaling in driving binge drinking behavior in females. We found that estrous cycle status dictates varying behavioral phenotypes in female mice, as females displayed greater binge alcohol drinking and reduced avoidance behavior when they were in a high ovarian E2 state than when they were in a low ovarian E2 state (**Fig. 1**). However, the mechanisms driving these effects diverged, as rapid E2 signaling was required for the pro-alcohol drinking, but not anxiolytic, effects of high ovarian E2 (**Figs. 3 & 4**). Intra-BNST E2 signaling, including that which could only signal at the cell membrane (mem-E2), rapidly promoted binge alcohol drinking in low E2 females (**Fig. 3f,g**). ERα, which was densely expressed within BNST glutamatergic circuit components, mediated the rapid pro-drinking effects of E2 (**Fig. 4**), altogether suggesting that nongenomic E2 signaling at membrane-associated ERα in the BNST mediates the pro-drinking effects of ovarian E2. Both high ovarian E2 state and acute E2 application in low ovarian E2 state females enhanced the synaptic excitation of a large subpopulation of $BNST^{CRF}$ neurons (**Fig. 2**; **Fig. 3j-m**), and this neuron population's activity was necessary for binge alcohol drinking, but not avoidance behavior, and enhanced by high E2 to drive motivated binge alcohol drinking (**Fig. 2**).

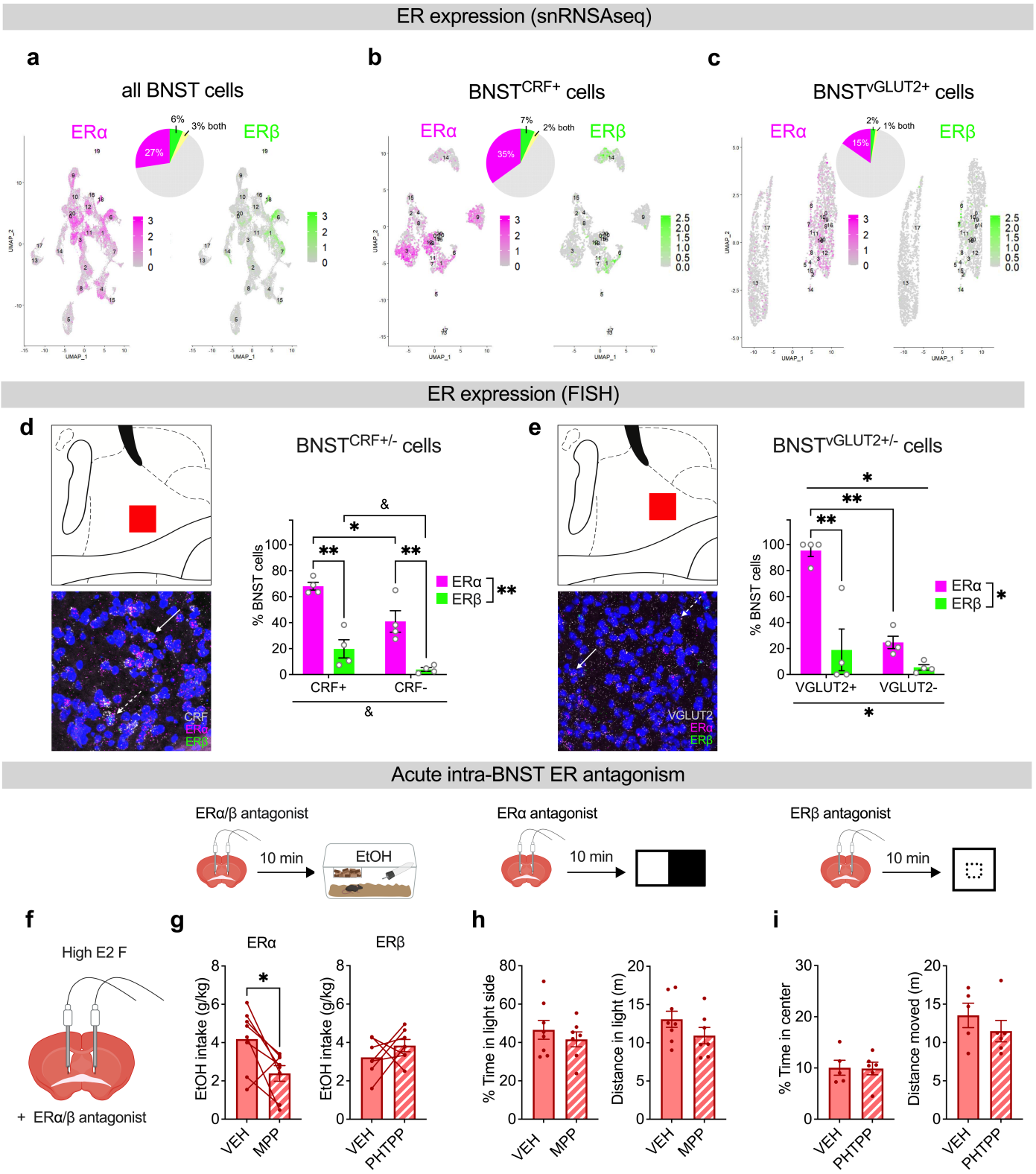

Figure 4: ERα is robustly expressed in the BNST and mediates rapid E2 modulation of binge drinking but not avoidance behavior. a-c) Analysis of single nucleus RNA sequencing (snRNA-seq) of female mouse BNST nuclei (total cells: 38,806; GEO: GSE126836)[77]. **a)** BNST cells expressing estrogen receptor α (ERα; *Esr1*, 27%) and estrogen receptor β (ERβ; *Esr2;* 6%) and both (3%). **b)** *Crh*-expressing BNST cells ($BNST^{CRF}$) expressing ERα (35%), ERβ (7%), and both (2%). **c)** *Slc17a6*-expressing BNST cells ($BNST^{VGLUT2}$) expressing ERα (15%), ERβ (2%), and both (1%). **d-e)** RNAscope fluorescence in situ hybridization (FISH) probing for ERα (*Esr1*) and ERβ (*Esr2*) in BNST cell types in females, with red boxes within schematics indicating representative area of confocal z-stack images taken (top left) and maximum projection images of z-stacks with channels pseudocolored for visibility (bottom left). **d)** ERα was expressed in more CRF+ cells than ERβ, with overall higher ERα expression in BNST CRF+ compared to CRF- cells. Solid arrow: cell

expressing CRF/ERα/ERβ; dashed arrow: cell expressing CRF/ERα. **e)** ERα was expressed in more VGLUT2+ cells than ERβ, with overall higher ERα expression in BNST VGLUT2+ compared to CRF- cells, showing a similar pattern to snRNA-seq expression. Solid arrow: cell expressing VGLUT2/ERα/ERβ; dashed arrow: cell expressing VGLUT2/ERα. **f–i)** Effects of acute intra-BNST ERα/β antagonism on behavior in high ovarian E2 status females. **f)** Depiction of strategy to site-deliver the ERα antagonist methyl-piperidino-pyrazole (MPP; 10 uM/200 nl/side), ERβ antagonist 4-[2-phenyl-5,7-bis(trifluoromethyl)pyrazolo[1,5-a]pyrimidin-3-yl]phenol (PHTPP; 10 uM/200 nl/side), or saline vehicle (VEH) to the BNST in high E2 females via bilateral indwelling cannulae 10 min prior to behavioral testing. **g)** ERα antagonism via intra-BNST MPP reduced binge drinking in high ovarian E2 females, with no effect of ERβ antagonism with PHTPP. **h)** ERα antagonism via intra-BNST MPP had no effect on avoidance behavior in the light/dark box (LDB). **i)** ERβ antagonism via intra-BNST PHTPP had no effect on avoidance behavior in the open field (OF). *P < 0.05, **P < 0.01, ***P < 0.001; 2xANOVA main effects and interactions between receptors; paired t-tests between VEH vs. ER antagonist treatment prior to DID; unpaired t-tests between VEH vs. ER antagonist treatment prior to avoidance assays; post hoc t-tests with H-S corrections as indicated. All schematics created with biorender.com.

There is significant evidence of an association between E2 and alcohol consumption in human[47,78], but associations between drinking and menstrual status have proven to be difficult to parse[79]. Careful monitoring of menstrual cycle stage and ovarian hormone status in nonhuman primates has been able to demonstrate that alcohol intake is modulated by fluctuating ovarian hormones across the menstrual cycle[80]. Previous work has shown that psychostimulant[32,81] and opioid[82]-related behaviors are modulated across the estrous cycle in rodents, however demonstrating estrous cycle modulation of alcohol drinking has proven to be challenging[9,52,83-85]. Nonetheless, many studies report that ovariectomy reduces alcohol intake[9,86] and E2 can enhance drinking in ovariectomized[9,56] and intact animals[57], suggesting a role for fluctuating E2 across the intact female rodent estrous cycle in alcohol drinking. Here, we validated a precise and accurate method for longitudinal monitoring of ovarian E2 status in intact female mice during behavior that allowed females to cycle normally. Using this, we provide the first evidence for a causal role of fluctuating E2 across the estrous cycle in alcohol drinking behavior in individual animals. In addition, we provide mechanistic insight into the role of ovarian E2 in alcohol drinking, showing that E2 signaling at membrane-associated ERα in the BNST is necessary and sufficient to drive binge alcohol drinking behavior. As males also have robust expression of ERs in the BNST that mediate behavior[19], locally aromatized E2 in the BNST may be able to regulate binge alcohol drinking in males through a similar E2-dependent mechanism. This may be similar to what has been described for rapid E2 synthesis and signaling modulation of birdsong and reproduction in birdsong and hypothalamic nuclei in birds[28,31,87].

Although the link between rapid E2 signaling and behavioral control has not previously been described in gonadally intact female rodents, there is a rich literature detailing signaling mechanisms of membrane-associated ER signaling[87-90]. Here, we find that rapid E2 signaling at membrane-associated receptors promotes synaptic excitation of $BNST^{CRF}$ neurons that are required for motivated alcohol drinking and more engaged when females are in a high ovarian E2 state. Similar to our finding that E2 increases glutamatergic synaptic transmission at $BNST^{CRF}$ synapses, it has been shown to enhance excitatory neurotransmission and excitation in the hippocampus and hypothalamus via mechanisms such as increasing glutamate release, dendritic spine formation, and long term potentiation[21,75,91,92].The current reports on the role of rapid E2 in behavioral control show that social memory is dependent on rapid-E2 mediated ERK and PI3K actions in the hippocampus[22], and E2-mediated enhancement of cocaine self-administration requires mGluR5 activity in ovariectomized females[93], indicating the importance of excitatory synaptic transmission in E2's behavioral role. Future work is necessary to fully elucidate the signaling mechanism underlying the role of rapid E2 in driving $BNST^{CRF}$ neuron activity to drive motivated alcohol drinking. Intriguingly, while our data show that only rapid E2 signaling is needed for ovarian E2's role in alcohol drinking, they indicate that high ovarian E2-mediated anxiolysis may require E2-dependent transcriptional programming in the BNST and/or other brain regions. Indeed, others have recently reported that chronic E2 treatment in ovariectomized female rats had no effect on avoidance behavior[70], suggesting that other estrous cycle-related hormones may be at play in intact females. These results further our understanding of the mechanisms driving early alcohol drinking and states of anxiety in females, a critical step in developing effective interventions to minimize long-term negative health outcomes of alcohol drinking, especially in females.

Methods

Subjects

All experimental mice were male and female mice on a C57BL/6J background strain and ≥ 10 wks of age. Wildtype (WT) adult male and female C57BL/6J mice were purchased from Jackson Laboratory (Bar Harbor, ME, USA) at 8 weeks of age and all transgenic lines were bred in our animal facility. CRF-ires-Cre (CRF-Cre) [73,94] mice were bred with WT C57BL/6J mice, and hemizygous CRF-Cre mice were bred with homozygous floxed Ai9-tdTomato mice purchased from Jackson Laboratory to produce CRF-Cre-reporter mice. All mice were housed under a reverse circadian 12 h:12 h light:dark cycle with lights off at 7:30 am and *ad libitum* access to food and water. Mice were singly housed at least one week prior to behavioral testing and remained singly housed throughout the experimental procedures. Experiments began approximately 3 hrs into the dark phase of the light:dark cycle. All procedures were conducted with approval of the Institutional Animal Care and Use Committee at Weill Cornell Medicine following the guidelines of the NIH Guide for the Care and Use of Laboratory Animals.

Estrous cycle monitoring

Estrous cycle stage was determined via daily lavage adapted from Mclean et al. [95], in which vaginal epithelial cells were collected with 15 µL 0.45% saline onto glass slides 1.5 hrs into the dark cycle and analyzed for cell types corresponding to the different estrous cycle stages (depicted in **Fig. 1a**; proestrus: high proportion of round nucleated cells; estrus: cornified cells; metestrus: low proportion of round nucleated cells and high proportion of cornified cells; diestrus: high proportion of round nucleated cells and high proportion of cornified cells).

Tissue and plasma collection

Naïve female mice estrous cycles were tracked daily for at least two weeks. Following prolonged tracking, mice categorized via cytology as being in either the proestrus (high E2 ovarian status) or metestrus (low E2 ovarian status) stages were rapidly decapitated under isoflurane anesthesia. Whole blood was collected from the trunk into tubes precoated with K_2EDTA (BD Microtainer). The whole blood was immediately spun down in a standard centrifuge at 1,500 x g for 10 mins at 4°C. The resulting plasma was collected and stored at -80°C until further analysis. Simultaneously, ovaries were dissected, frozen immediately on dry ice, and stored at -80°C.

Plasma estrogen concentration measurement

17β-Estradiol (E2) was quantified in pooled plasma samples by liquid chromatography-triple quadrupole tandem mass spectrometry (LC-MS/MS) using slight modifications of methods described previously[96]. Standard solutions of E2 (1.000 ± 0.005 mg/ml) and estradiol-2,4,16,16,17-d5 (E2-d5; 100 µg/ml) were obtained from Cerilliant (Round Rock, TX, USA) as 1 ml ampules with acetonitrile (ACN) as solvent. Charcoal-stripped human serum (CSS; Mass Spect Gold MSG3100, Golden West Biologicals, Temecula, CA, USA) was spiked with a working E2 standard stock (2 µg/ml) using a Hamilton syringe to yield a high calibration standard with a final E2 concentration of 4 ng/ml. Two-fold serial dilutions of the high calibration standard were prepared in CSS to yield 14 calibration standards including a blank (0 ng/ml). Three in-house serum pools (2 human, 1 nonhuman primate) were used as quality control (QC) samples. Calibration standards, QC samples, and pooled plasma samples (150 µl) were reverse-pipetted into 350 µl V-bottom 96-well microtiter plates (Shimadzu, Kyoto, Japan) followed by the addition of 100 µl of an internal standard spike (3.7 ng/ml E2-d5) into each well. Plates were shaken on an orbital shaker at room temperature for 1 hr and the contents of each well were transferred to 400 µl 96-well Isolute SLE+ plates (Biotage, Uppsala, Sweden) that had been washed with dichloromethane (DCM; 6 x 600 µl) and allowed to completely dry. Plates were equilibrated at room temperature for five min then eluted with DCM (3 x 600 µl) into 2 ml 96-well round bottom polypropylene plates (Analytical Sales & Services, Flanders, NJ, USA) containing 100 µl of 2-propanol per well. Plates were then subjected to positive pressure (~5 psi, 60 s) using a Pressure+ 96 positive pressure manifold (Biotage) to elute residual eluent. Eluates were evaporated to dryness under nitrogen at 40°C using a TurboVap 96 evaporation system (Biotage) and samples were reconstituted in 50 µL of 25:75 methanol:water (v/v) and transferred to new 350 µl V-bottom 96-well microtiter plates for analysis.

LC-MS/MS analysis was performed on a Shimadzu LCMS-8060 system. Twenty-five microliters of each reconstituted sample were injected from the microtiter plate (held at 10°C) onto a Raptor Biphenyl column (100 mm x 2.1 mm x 2.7 µm particle size; Restek, Bellefonte, PA, USA) with guard cartridge (5 mm x 2.1 mm x 2.7 µm particle size; Restek) held at 35°C. Analytes were eluted with an eluent gradient initially consisting of 35% mobile phase A (0.15 mM ammonium fluoride in water) and 65% mobile phase B (pure methanol) that was

linearly changed to 97% B over 4 min and then to 100% B over 1.1 min. The column was then washed with 100% B for 1.8 min before being returned to 65% B over 0.1 min and allowed to equilibrate for 3.4 min, for a total method time of 10.4 min. The flow rate was held constant at 0.4 ml/min. Analytes were detected via heated electrospray ionization in negative ionization mode with scheduled multiple reaction monitoring (E2: 271.05 > 145.05 quantifier, > 143.05 reference; E2-d5: 276.20 > 187.10 quantifier, > 147.10 reference). Heating gas (air; 10 L/min), drying gas (nitrogen; 10 L/min), and nebulizing gas (nitrogen; 3 L/min) were provided by a Peak Genius 1051 gas generator (Peak Scientific, Inchinnan, Scotland, UK). The interface temperature was 300°C, the heat block temperature was 400°C, and the desolvation line temperature was 250°C. Argon (Airgas) at 320 kPa was used as the collision gas. The source was equipped with a capillary B needle (Shimadzu) and capillary protrusion and probe distance were determined empirically based on maximizing E2 response. Shimadzu Lab Solutions software (version 5.97) was used to optimize the quadrupole pre-bias voltages and collision energies; the interface voltage -2 kV. The calibration curve was constructed using linear regression with 1/C weighting of the analyte/internal standard peak area ratio. The lower limit of quantification (LLOQ) for E2 was 1 pg/ml, defined as the lowest calibration curve concentration having an average accuracy of 80–120% and a CV of <20%[97].

Western immunoblotting

Tissue was homogenized using a Teflon pestle (Pyrex, Illinois, USA) in cold RIPA buffer (Pierce, Massachusetts, USA) containing protease and phosphatase inhibitors. After spinning the homogenate at 12000 × g for 20 min, the supernatant was collected and used for western immunoblotting. Twenty µg of protein per sample were separated by 10% SDS-PAGE and transferred to polyvinylidene difluoride membranes, which were blocked in 5% nonfat dry milk and incubated 24-73 h at 4 °C in a primary antibody prior to being incubated in peroxidase-linked IgG conjugated secondary antibody at 1:5000 at room temperature for 1 h. Blots were incubated with AROM (Invitrogen, California, USA) diluted to 1:1000 and GAPDH (Abcam, Cambridge, UK) diluted to 1:40000. Proteins were quantified at the following molecular weights: AROM at 55 kDa and GAPDH at 36 kDa. Protein bands were quantified as mean optical intensity using ImageJ software (NIH) and normalized to GAPDH. Normalized optical density values from each sample were used to calculate the fold change for each proestrus group compared with the metestrus group (set to 1.0) on the same blot.

Single nucleus RNA sequencing

Gene-expression matrices from female mouse BNST samples from dataset GEO: GSE126836[77] were loaded into R (v 4.3.1) [98] and preprocessed using Seurat[99]. We normalized the data using *NormalizeData.* Variable features were found using *FindVariableFeatures* using the vst selection method and nfeatures = 2000. Cells expressing genes of interest were subsetted and clustered. UMAPs showing co-expression of genes were generated with *FeaturePlot.*

RNAscope fluorescence *in situ* hybridization

Mice were euthanized under deep isoflurane anesthesia and their brains rapidly extracted, flash frozen in -35 °C 2-methylbutane, and stored at -80 °C under RNase-free conditions. Brains were embedded in OCT blocks with four brains per block, and 20 µM coronal sections were sliced on a cryostat and collected onto Superfrost Plus slides and stored at -80 °C in sealed slide boxes until undergoing *in situ* hybridization. Slides were thawed and in situ hybridization was conducted per manufacturer instructions using RNAscope Multiplex Fluorescent v1 kit with the HybEZ Oven and the following ACD probes: VGLUT2: mm-Slc17a6, cat #319171; CRF: mm-Crh, cat #316091; ERa: mm-Esr1, cat #478201; ERb: mm-Esr2, cat #316121. Slides were counterstained with DAPI and cover slipped with Vectashield. Images were acquired on a Zeiss LSM 880 Laser Scanning Confocal microscope in 1 µM plane z-stacks and manually analyzed in Metamorph according to RNAscope instructions to quantify the number of DAPI+ nuclei and number of DAPI+ cells expressing each probe alone or in combination. Representative images (**Fig. 4d,e**) were pseudocolored following analysis for color matching purposes using ImageJ (1.53a).

Drugs

Cyclodextrin-encapsulated E2 (Millipore Sigma, Massachusetts, USA) was dissolved in 0.9% saline, letrozole (LET; Tocris Bioscience, Bristol, UK) was dissolved in 5% dimethyl sulfoxide in 0.9% saline. MPP dichloride and PHTPP (Tocris Bioscience) were dissolved in 1% dimethyl sulfoxide and 0.9% saline. Membrane-only E2 (E2-BSA; Steraloids, Rhode Island, USA) was purified using Zeba™ Spin Desalting Columns, 7K (Thermo-Fischer, Massachusetts, USA) as follows: the column's storage solution was removed by centrifugal spinning

at 1500 x g for 1 min, then the column was conditioned with phosphate buffered saline (300 µl x 3). Membrane-only E2 (approx. 2 mg/min in phosphate buffered saline, 120 µl) was loaded and eluted by centrifugal spinning at 1500 x g for 2 min. The exact concentration (36 µM) was assessed using BCA protein assay.

Stereotaxic surgery

For experiments requiring site-directed administration of viral vectors or cannulae implantation, mice were anesthetized with 2% isoflurane (VetEquip, CA, USA) in 0.8% oxygen in an induction chamber (VetEquip,) then placed in an Angle Two mouse stereotaxic frame (Leica Biosystems, Wetzlar, Germany) and secured with ear bars into a nose cone delivering isoflurane to maintain anesthesia. Mice were given a subcutaneous injection of meloxicam (2 mg/kg) for preemptive analgesia and 0.1 mL of 0.25% Marcaine around the incision site. For administration of viral vectors, a Neuros 7000 series 1 µL Hamilton syringe with a 33-gauge needle (Reno, NV) connected to a remote automated microinfusion pump (KD Scientific, Holliston, MA) was used for construct delivery at a rate of 50–100 nL/min to the BNST (A/P: +0.3 mm, M/L: ±1.1 mm, D/V: −4.35 mm, 250 nL). Following infusion, the needle was left in place for 10 min and then slowly manually retracted to allow for diffusion and prevent backflow of the virus. Mice were continuously monitored for at least 30 min post-surgery to ensure recovery of normal breathing pattern and sternal recumbency and then checked daily. For cannulae implantation surgeries, bilateral cannulae (P Technologies, Virginia, USA) cut to 2.2 mm below the pedestal were secured with C & B Metabond dental cement at the same BNST coordinates used for viral infusions. The cannulae were secured with an internal dummy and plastic dust cap (P Technologies). For cannula histologies, mice were deeply anesthetized with isoflurane and 200 nL dye (Chicago Sky, Millipore Sigma) was infused. Brains were rapidly extracted from anesthetized animals and flash frozen, embedded in OTC, and sectioned at 45 µm on the cryostat to ensure placement of cannula. DREADD and fiber photometry brains were extracted, post-fixed overnight in 4% PFA, and then placed in PBS until they were sliced on the coronal plane in 45 µm sections on a VT1000S vibratome (Leica Biosystems, Wetzlar, Germany) to check injection placements and viral expression.

Behavior assays

Drinking in the Dark

The Drinking in the Dark (DID) binge alcohol drinking paradigm was used to model human binge consumption behavior in mice as previously described[49,100]. On Days 1-3 of each cycle of alcohol DID, three hrs into the dark cycle, the home cage water bottle was replaced with a bottle containing 20% (v/v) ethanol for two hrs and four hrs on Day 4, followed by three days of abstinence between cycles. The same schedule was used to evaluate binge sucrose consumption, except that home cage water bottles were replaced with 1% (w/v) sucrose. For all drinking experiments, empty “dummy” cages on the same rack as behavior mice received the same alcohol or sucrose bottle replacement, and consumption was adjusted for a leak from dummy bottles and then normalized to bodyweight.

Avoidance behavior

Avoidance behavior was assessed as previously described[64,73]. SMART software (Panlab, Barcelona, Spain) and Ethovision 15 (Noldus, Wageningen, Netherlands) video tracking were used to quantify raw locomotor and location data used to calculate measures including distance traveled and time spent. For basal avoidance behavior (**Fig. 1i-m**), assays were performed once per week within the same cohorts of mice.

<u>Open field test</u>

The open field test (OF) was conducted in a novel 50 × 50 cm plexiglass arena. Mice were placed in a corner of the arena, and time and distance in the center 50% of the apparatus vs. corners and periphery across the 60 min trial were calculated.

<u>Elevated plus maze</u>

The elevated plus maze (EPM) was conducted in a plexiglass maze with two open and two closed arms (35 cm length × 5.5 cm width, with walls 15 cm tall in the closed arms). Mice were placed in the center of the EPM and time and distance in the open arms, closed arms, and center platform were calculated for the five min trial.

<u>Light/Dark Box</u>

The light/dark box assay (LDB) was conducted in a rectangular box divided into two equal compartments (20 cm l × 40 cm w × 34.5 cm h) with one dark with a closed lid and the other with an open top and illuminated by

two 60 W bulbs placed 30 cm above the box. The two compartments were separated by a divider with a 6 cm x 6 cm cut-out passageway at floor level. The mouse was placed in a corner of the light compartment and allowed to freely explore the apparatus, and the number of light side entries and time spent in the light vs. dark compartment were calculated for the 10 min trial.

Pharmacological manipulations

Systemic LET (1 or 10 mg/kg) or vehicle control were administered via intraperitoneal (i.p.) injection 40 min prior to alcohol or sucrose bottles being placed in the cages. For central infusions via cannulation, cyclodextrin-encapsulated E2 (20 pg), membrane-only E2 (55 pg), MPP (10 uM), or PHTPP (10 uM) in a total volume of 200 nL was infused bilaterally into BNST targeted guide cannulae using two Neuros 7000 series 1 µL Hamilton syringes with 33-gauge needles attached to a Harvard Apparatus pump. Ten mins following BNST infusion, DID ethanol or sucrose bottles were placed into cages for DID or mice were placed in the testing apparatuses for avoidance assays.

Chemogenetic manipulations

CRF-Cre mice were injected with a cocktail of viral vectors containing Cre-dependent excitatory and inhibitory Designer Receptors Exclusively Activated only by Designer Drugs (DREADDs) (1:1 cocktail of the excitatory Gq-DREADD AAV2-hSyn-DIO-hM3D[Gq]-mCherry [125 nL] plus inhibitory Gi-KORD AAV8-hSyn-DIO-KORD[Gi]-mCitrine [125 nL]) or control virus (AAV2-hSyn-DIO-mCherry [250 nL]) in the BNST. After three weeks to allow for viral expression, mice underwent behavioral tests (conducted under 200-250 lux lighting conditions) to evaluate the role of the $BNST^{CRF}$ neurons in mediating avoidance behaviors and alcohol DID, All behavioral experiments/drinking sessions commenced three hrs into the dark cycle, and each avoidance behavioral apparatus was thoroughly cleaned with 70% ethanol before each trial. For chemogenetic manipulation experiments, mice received vehicle (0.9% sterile saline, i.p.) or DREADD ligand dissolved in vehicle (CNO, 5 mg/kg, i.p., or SalB, 10-17 mg/kg, i.p.) injections 10-40 min prior to behavioral testing.

Fiber photometry

CRF-Cre mice expressing GCaMP6s in the BNST and a permanent fiber cannula implanted above the BNST were first habituated to handling and tethering of fiber optic patch cables during the week prior to the avoidance behavioral assays. Optical patch cables were photobleached through the fiber photometry workstation (Tucker-Davis Technologies, Inc., Alachua, Florida) for at least 12 hr prior to being tethered to the mouse's head stage prior to each behavioral session. For drinking experiments, mice underwent a modified DID procedure in which they received water access prior to and after each 2-hr alcohol access. Drinking was measured using a capacitance based lickometer that elicited a TTL signal when licked, and a drinking bout was defined as at least 2 TTL pulses within one s, with a minimum bout length of 0.5 s. Raw fiber photometry signals (465 nm channel for GCaMP, 405 nm channel for the isosbestic point control) were collected at a sampling rate of 1017.25 Hz and denoised using a median filter to remove electrical artifacts and a lowpass filter to reduce high-frequency noise. To eliminate noise in the signal due to transfer to the behavioral apparatus or associated with bottle changes, the first 150 s for EPM, 400 s excluded for OF, and 1000 s for DID were excluded from analysis. The EPM trial length was increased to provide 5 min of analyzed data. The preprocessed data were downsampled by factor of 100 and corrected for photobleaching and motion artifacts by finding the best linear fit of the isosbestic control signal to the GCaMP signal and subtracting this estimated motion component from the GCaMP signal. Final z-score values were calculated by subtracting the mean of the whole trace from each datapoint and dividing it by the standard deviation of the trace. Data were analyzed based on behavioral epoch or tracked location.

***Ex vivo* slice electrophysiology**

CRF-Cre reporter mice[37] were rapidly decapitated under isoflurane anesthesia and their brains extracted. Brains were blocked on the coronal plane and acute 300 µm coronal slices prepared and incubated in carbogenated solutions with a pH of 7.35 and osmolarity of 305 as previously described[41]. Sections including BNST were sliced in N-methyl-D-glucamine (NMDG) artificial cerebrospinal fluid (NMDG-aCSF) at RT containing (in mM): 92 NMDG, 2.5 KCl, 1.25 NaH_2PO_4, 30 $NaHCO_3$, 20 HEPES, 25 glucose, 2 thiourea, 5 Na-ascorbate, 3 Na-pyruvate, 0.5 $CaCl_2 \cdot 2H_2O$, and 10 $MgSO_4 \cdot 7H_2O$. Slices were transferred to NMDG-aCSF at 32°C for 12-14 min, and then incubated for at least 1 hr at RT in HEPES-aCSF containing (in mM): 92 NaCl, 2.5 KCl, 1.25 NaH_2PO_4, 30 $NaHCO_3$, 20 HEPES, 25 glucose, 2 thiourea, 5 Na-ascorbate, 3 Na-pyruvate, 2 $CaCl_2 \cdot 2H_2O$, and 2 $MgSO_4 \cdot 7H_2O$. Slices were placed in the recording chamber and perfused at a rate of 2

ml/min with 30°C normal aCSF containing (in mM): 124 NaCl, 2.5 KCl, 1.25 NaH_2PO_4, 24 $NaHCO_3$, 12.5 glucose, 5 HEPES, 2 $CaCl_2$·2H2O, and 2 $MgSO_4$·$7H_2O$, for at least 20 min prior to electrophysiological recordings. CRF+ (tdTomato-tagged) neurons were visualized using a 560 nm LED and 40× immersed objective with DsRed filter14. Spontaneous excitatory postsynaptic currents (sEPSCs, 2 cells/mouse) were measured in a voltage clamp configuration using a cesium-gluconate-based intracellular recording solution containing (in mM): 117 D-gluconic acid, 20 HEPES, 0.4 EGTA, 5 TEA, 2 $MgCl_2$-$6H_2O$, 4 Na-ATP and 0.4 Na-GTP (pH 7.3 and 290 mOsm),) and a holding potential of -70 mV, using picrotoxin (25 μM) in the bath to block GABAergic synaptic transmission. E2 in aCSF (1 nM, 10 nM, 100 nM, 1000 nM) was washed on to measure its effect on excitatory synaptic transmission. Responder category threshold was defined as 15% delta of average E2 wash on period OR 50% delta in a one min period during E2 wash on. Signals were acquired using a Multiclamp 700B amplifier (Molecular Devices), digitized, and analyzed via pClamp 10.4 or 11 software (Molecular Devices). Input resistance and access resistance were continuously monitored throughout experiments, and cells in which properties changed by more than 20% were not included in data analysis.

Statistical analyses

Statistical analyses were performed in GraphPad Prism 10. Data in each group for all dependent measures were checked for their distributions in raw and log space within the group and equality of variance across groups and analyzed accordingly. Statistical comparisons were always performed with an alpha level of 0.05 and using two-tailed analyses. Paired t-tests for within-subjects and unpaired t-tests for between-subjects direct comparisons were used to evaluate the effects of E2 modulators on alcohol drinking and avoidance behaviors. Two-way and three-way repeated measures ANOVAs (RM-ANOVAs) were used to examine the effects of cycle, groups, and drug and other repeated variables between mice in different experimental conditions; mixed effects models were used when one or more matched data point was unavailable. Following significant effects in ANOVAs, *post hoc* direct comparisons were performed using unpaired or paired t-tests with Holm-Sidak (H-S) correction for multiple comparisons, and adjusted p values are reported. Linear regressions were performed for correlation analyses. Data in figures are presented as mean ± SEM, and raw data points are included in all figures except some repeated measures graphs in which there were too many raw data points to be clearly represented.

Data availability

All raw and analyzed data will be made publicly available and accession codes provided prior to publication.

Code availability

All custom code written in MATLAB, R, and Python will be publicly deposited on GitHub prior to publication.

References

1 Galea, L. A. M., Frick, K. M., Hampson, E., Sohrabji, F. & Choleris, E. Why estrogens matter for behavior and brain health. *Neurosci Biobehav Rev* **76**, 363-379 (2017). https://doi.org/10.1016/j.neubiorev.2016.03.024

2 Simpson, E. R. Sources of estrogen and their importance. *J Steroid Biochem Mol Biol* **86**, 225-230 (2003). https://doi.org/10.1016/s0960-0760(03)00360-1

3 Findlay, J. K., Liew, S. H., Simpson, E. R. & Korach, K. S. Estrogen signaling in the regulation of female reproductive functions. *Handb Exp Pharmacol*, 29-35 (2010). https://doi.org/10.1007/978-3-642-02062-9_2

4 Taxier, L. R., Gross, K. S. & Frick, K. M. Oestradiol as a neuromodulator of learning and memory. *Nat Rev Neurosci* **21**, 535-550 (2020). https://doi.org/10.1038/s41583-020-0362-7

5 Frick, K. M. & Kim, J. Mechanisms underlying the rapid effects of estradiol and progesterone on hippocampal memory consolidation in female rodents. *Horm Behav* **104**, 100-110 (2018). https://doi.org/10.1016/j.yhbeh.2018.04.013

6 Sharma, R., Cameron, A., Fang, Z., Ismail, N. & Smith, A. The regulatory roles of progesterone and estradiol on emotion processing in women. *Cogn Affect Behav Neurosci* **21**, 1026-1038 (2021). https://doi.org/10.3758/s13415-021-00908-7

7 Albert, K. M. & Newhouse, P. A. Estrogen, Stress, and Depression: Cognitive and Biological Interactions. *Annu Rev Clin Psychol* **15**, 399-423 (2019). https://doi.org/10.1146/annurev-clinpsy-050718-095557

8 Johnson, C. S. & Mermelstein, P. G. The interaction of membrane estradiol receptors and metabotropic glutamate receptors in adaptive and maladaptive estradiol-mediated motivated behaviors in females. *Int Rev Neurobiol* **168**, 33-91 (2023). https://doi.org/10.1016/bs.irn.2022.11.001

9 Satta, R., Hilderbrand, E. R. & Lasek, A. W. Ovarian Hormones Contribute to High Levels of Binge-Like Drinking by Female Mice. *Alcohol Clin Exp Res* **42**, 286-294 (2018). https://doi.org/10.1111/acer.13571

10 Marino, M., Galluzzo, P. & Ascenzi, P. Estrogen signaling multiple pathways to impact gene transcription. *Curr Genomics* **7**, 497-508 (2006). https://doi.org/10.2174/138920206779315737

11 Kelly, M. J. & Rønnekleiv, O. K. Membrane-initiated estrogen signaling in hypothalamic neurons. *Mol Cell Endocrinol* **290**, 14-23 (2008). https://doi.org/10.1016/j.mce.2008.04.014

12 Tozzi, A., Bellingacci, L. & Pettorossi, V. E. Rapid Estrogenic and Androgenic Neurosteroids Effects in the Induction of Long-Term Synaptic Changes: Implication for Early Memory Formation. *Front Neurosci* **14**, 572511 (2020). https://doi.org/10.3389/fnins.2020.572511

13 Yoest, K. E., Quigley, J. A. & Becker, J. B. Rapid effects of ovarian hormones in dorsal striatum and nucleus accumbens. *Horm Behav* **104**, 119-129 (2018). https://doi.org/10.1016/j.yhbeh.2018.04.002

14 Evans, P. D. Rapid signalling responses via the G protein-coupled estrogen receptor, GPER, in a hippocampal cell line. *Steroids* **152**, 108487 (2019). https://doi.org/10.1016/j.steroids.2019.108487

15 Qiu, J., Rønnekleiv, O. K. & Kelly, M. J. Modulation of hypothalamic neuronal activity through a novel G-protein-coupled estrogen membrane receptor. *Steroids* **73**, 985-991 (2008). https://doi.org/10.1016/j.steroids.2007.11.008

16 Subbamanda, Y. D. & Bhargava, A. Intercommunication between Voltage-Gated Calcium Channels and Estrogen Receptor/Estrogen Signaling: Insights into Physiological and Pathological Conditions. *Cells* **11** (2022). https://doi.org/10.3390/cells11233850

17 Huang, G. Z. & Woolley, C. S. Estradiol acutely suppresses inhibition in the hippocampus through a sex-specific endocannabinoid and mGluR-dependent mechanism. *Neuron* **74**, 801-808 (2012). https://doi.org/10.1016/j.neuron.2012.03.035

18 Trainor, B. C., Lin, S., Finy, M. S., Rowland, M. R. & Nelson, R. J. Photoperiod reverses the effects of estrogens on male aggression via genomic and nongenomic pathways. *Proceedings of the National Academy of Sciences of the United States of America* **104**, 9840-9845 (2007). https://doi.org/10.1073/pnas.0701819104

19 Trainor, B. C., Finy, M. S. & Nelson, R. J. Rapid effects of estradiol on male aggression depend on photoperiod in reproductively non-responsive mice. *Hormones and behavior* **53**, 192-199 (2008). https://doi.org/10.1016/j.yhbeh.2007.09.016
20 Cross, E. & Roselli, C. E. 17beta-estradiol rapidly facilitates chemoinvestigation and mounting in castrated male rats. *Am J Physiol* **276**, R1346-1350 (1999). https://doi.org/10.1152/ajpregu.1999.276.5.R1346
21 Phan, A. *et al.* Rapid increases in immature synapses parallel estrogen-induced hippocampal learning enhancements. *Proc Natl Acad Sci U S A* **112**, 16018-16023 (2015). https://doi.org/10.1073/pnas.1522150112
22 Sheppard, P. A. S. *et al.* Social memory in female mice is rapidly modulated by 17β-estradiol through ERK and Akt modulation of synapse formation. *Proc Natl Acad Sci U S A* **120**, e2300191120 (2023). https://doi.org/10.1073/pnas.2300191120
23 Becker, J. B. Estrogen rapidly potentiates amphetamine-induced striatal dopamine release and rotational behavior during microdialysis. *Neurosci Lett* **118**, 169-171 (1990). https://doi.org/10.1016/0304-3940(90)90618-j
24 Hu, M. & Becker, J. B. Effects of sex and estrogen on behavioral sensitization to cocaine in rats. *J Neurosci* **23**, 693-699 (2003). https://doi.org/10.1523/JNEUROSCI.23-02-00693.2003
25 Hu, M., Crombag, H. S., Robinson, T. E. & Becker, J. B. Biological basis of sex differences in the propensity to self-administer cocaine. *Neuropsychopharmacology* **29**, 81-85 (2004). https://doi.org/10.1038/sj.npp.1300301
26 Taziaux, M., Keller, M., Bakker, J. & Balthazart, J. Sexual behavior activity tracks rapid changes in brain estrogen concentrations. *J Neurosci* **27**, 6563-6572 (2007). https://doi.org/10.1523/JNEUROSCI.1797-07.2007
27 Cornil, C. A., Taziaux, M., Baillien, M., Ball, G. F. & Balthazart, J. Rapid effects of aromatase inhibition on male reproductive behaviors in Japanese quail. *Horm Behav* **49**, 45-67 (2006). https://doi.org/10.1016/j.yhbeh.2005.05.003
28 de Bournonville, M. P. *et al.* Rapid changes in brain estrogen concentration during male sexual behavior are site and stimulus specific. *Sci Rep* **11**, 20130 (2021). https://doi.org/10.1038/s41598-021-99497-1
29 Balthazart, J. *et al.* Rapid changes in production and behavioral action of estrogens. *Neuroscience* **138**, 783-791 (2006). https://doi.org/10.1016/j.neuroscience.2005.06.016
30 Remage-Healey, L., Coleman, M. J., Oyama, R. K. & Schlinger, B. A. Brain estrogens rapidly strengthen auditory encoding and guide song preference in a songbird. *Proc Natl Acad Sci U S A* **107**, 3852-3857 (2010). https://doi.org/10.1073/pnas.0906572107
31 Scarpa, G. B. *et al.* Estrogens rapidly shape synaptic and intrinsic properties to regulate the temporal precision of songbird auditory neurons. *Cereb Cortex* **33**, 3401-3420 (2023). https://doi.org/10.1093/cercor/bhac280
32 Quigley, J. A., Logsdon, M. K., Graham, B. C., Beaudoin, K. G. & Becker, J. B. Activation of G protein-coupled estradiol receptor 1 in the dorsolateral striatum enhances motivation for cocaine and drug-induced reinstatement in female but not male rats. *Biol Sex Differ* **12**, 46 (2021). https://doi.org/10.1186/s13293-021-00389-w
33 Tonn Eisinger, K. R., Gross, K. S., Head, B. P. & Mermelstein, P. G. Interactions between estrogen receptors and metabotropic glutamate receptors and their impact on drug addiction in females. *Horm Behav* **104**, 130-137 (2018). https://doi.org/10.1016/j.yhbeh.2018.03.001
34 Becker, J. B. & Rudick, C. N. Rapid effects of estrogen or progesterone on the amphetamine-induced increase in striatal dopamine are enhanced by estrogen priming: A microdialysis study. *Pharmacology Biochemistry and Behavior* **64** (1999).
35 Chen, H. *et al.* Effect of a brain-penetrant selective estrogen receptor degrader (SERD) on binge drinking in female mice. *Alcohol Clin Exp Res* (2022). https://doi.org/10.1111/acer.14874

36 Hilderbrand, E. R. & Lasek, A. W. Estradiol enhances ethanol reward in female mice through activation of ERα and ERβ. *Horm Behav* **98**, 159-164 (2018). https://doi.org/10.1016/j.yhbeh.2018.01.001
37 Koob, G. F. Alcoholism: allostasis and beyond. *Alcoholism, clinical and experimental research* **27**, 232-243 (2003).
38 Grant, B. F. *et al.* Prevalence of 12-Month Alcohol Use, High-Risk Drinking, and DSM-IV Alcohol Use Disorder in the United States, 2001-2002 to 2012-2013: Results From the National Epidemiologic Survey on Alcohol and Related Conditions. *JAMA Psychiatry* **74**, 911-923 (2017). https://doi.org/10.1001/jamapsychiatry.2017.2161
39 Vsevolozhskaya, O. A. & Anthony, J. C. Transitioning from First Drug Use to Dependence Onset: Illustration of a Multiparametric Approach for Comparative Epidemiology. *Neuropsychopharmacology* **41**, 869-876 (2016). https://doi.org/10.1038/npp.2015.213
40 Pollard, M. S., Tucker, J. S. & Green, H. D. Changes in Adult Alcohol Use and Consequences During the COVID-19 Pandemic in the US. *JAMA Netw Open* **3**, e2022942 (2020). https://doi.org/10.1001/jamanetworkopen.2020.22942
41 Weerakoon, S. M., Jetelina, K. K. & Knell, G. Longer time spent at home during COVID-19 pandemic is associated with binge drinking among US adults. *Am J Drug Alcohol Abuse* **47**, 98-106 (2021). https://doi.org/10.1080/00952990.2020.1832508
42 Ashley, M. J. *et al.* Morbidity in alcoholics. Evidence for accelerated development of physical disease in women. *Arch Intern Med* **137**, 883-887 (1977). https://doi.org/10.1001/archinte.137.7.883
43 Diehl, A. *et al.* Alcoholism in women: is it different in onset and outcome compared to men? *Eur Arch Psychiatry Clin Neurosci* **257**, 344-351 (2007). https://doi.org/10.1007/s00406-007-0737-z
44 Randall, C. L. *et al.* Telescoping of landmark events associated with drinking: a gender comparison. *J Stud Alcohol* **60**, 252-260 (1999). https://doi.org/10.15288/jsa.1999.60.252
45 Sarkola, T., Mäkisalo, H., Fukunaga, T. & Eriksson, C. J. Acute effect of alcohol on estradiol, estrone, progesterone, prolactin, cortisol, and luteinizing hormone in premenopausal women. *Alcohol Clin Exp Res* **23**, 976-982 (1999).
46 Muti, P. *et al.* Alcohol consumption and total estradiol in premenopausal women. *Cancer Epidemiol Biomarkers Prev* **7**, 189-193 (1998).
47 Martin, C. A., Mainous, A. G., Curry, T. & Martin, D. Alcohol use in adolescent females: correlates with estradiol and testosterone. *Am J Addict* **8**, 9-14 (1999). https://doi.org/10.1080/105504999306036
48 Strzelecki, A. M., Gipson, C. D., Childs, E. & Weafer, J. Preliminary evidence of increased alcohol use associated with ethinyl estradiol levels in women using oral contraceptives. *Drug Alcohol Depend Rep* **9**, 100194 (2023). https://doi.org/10.1016/j.dadr.2023.100194
49 Levine, O. B. *et al.* The paraventricular thalamus provides a polysynaptic brake on limbic CRF neurons to sex-dependently blunt binge alcohol drinking and avoidance behavior in mice. *Nat Commun* **12**, 5080 (2021). https://doi.org/10.1038/s41467-021-25368-y
50 Sneddon, E. A., White, R. D. & Radke, A. K. Sex Differences in Binge-Like and Aversion-Resistant Alcohol Drinking in C57BL/6J Mice. *Alcohol Clin Exp Res* **43**, 243-249 (2019). https://doi.org/10.1111/acer.13923
51 Li, J. *et al.* Differences between male and female rats in alcohol drinking, negative affects and neuronal activity after acute and prolonged abstinence. *Int J Physiol Pathophysiol Pharmacol* **11**, 163-176 (2019).
52 Priddy, B. M. *et al.* Sex, strain, and estrous cycle influences on alcohol drinking in rats. *Pharmacol Biochem Behav* **152**, 61-67 (2017). https://doi.org/10.1016/j.pbb.2016.08.001
53 Rivera-Irizarry, J. K. *et al.* Sex differences in binge alcohol drinking and the behavioral consequences of protracted abstinence in C57BL/6J mice. *Biol Sex Differ* **14**, 83 (2023). https://doi.org/10.1186/s13293-023-00565-0
54 Ford, M. M., Eldridge, J. C. & Samson, H. H. Ethanol consumption in the female Long-Evans rat: a modulatory role of estradiol. *Alcohol* **26**, 103-113 (2002).

55 Ford, M. M., Eldridge, J. C. & Samson, H. H. Determination of an estradiol dose-response relationship in the modulation of ethanol intake. *Alcoholism-Clinical and Experimental Research* **28**, 20-28 (2004). https://doi.org/10.1097/01.Alc.0000108647.62718.5a
56 Rajasingh, J. *et al.* Enhanced voluntary alcohol consumption after estrogen supplementation negates estrogen-mediated vascular repair in ovariectomized mice. *Endocrinology* **148**, 3618-3624 (2007). https://doi.org/10.1210/en.2006-1357
57 Quirarte, G. L. *et al.* Estradiol valerate and alcohol intake: dose-response assessments. *BMC pharmacology* **7**, 3 (2007). https://doi.org/10.1186/1471-2210-7-3
58 Kelly, D. A., Varnum, M. M., Krentzel, A. A., Krug, S. & Forger, N. G. Differential control of sex differences in estrogen receptor α in the bed nucleus of the stria terminalis and anteroventral periventricular nucleus. *Endocrinology* **154**, 3836-3846 (2013). https://doi.org/10.1210/en.2013-1239
59 Weiser, M. J., Foradori, C. D. & Handa, R. J. Estrogen receptor beta in the brain: from form to function. *Brain Res Rev* **57**, 309-320 (2008). https://doi.org/10.1016/j.brainresrev.2007.05.013
60 Logrip, M. L., Koob, G. F. & Zorrilla, E. P. Role of corticotropin-releasing factor in drug addiction: potential for pharmacological intervention. *CNS Drugs* **25**, 271-287 (2011). https://doi.org/10.2165/11587790-000000000-00000
61 Koob, G. F. Brain stress systems in the amygdala and addiction. *Brain Res* **1293**, 61-75 (2009). https://doi.org/10.1016/j.brainres.2009.03.038
62 Koob, G. F. Corticotropin-releasing factor, neuroplasticity (sensitization), and alcoholism. *Proc Natl Acad Sci U S A* **105**, 8809-8810 (2008). https://doi.org/10.1073/pnas.0804354105
63 Pleil, K. E. & Skelly, M. J. CRF modulation of central monoaminergic function: Implications for sex differences in alcohol drinking and anxiety. *Alcohol* **72**, 33-47 (2018). https://doi.org/10.1016/j.alcohol.2018.01.007
64 Rivera-Irizarry, J. K. *et al.* (BioRxiv, 2023).
65 Sneddon, E. A., Ramsey, O. R., Thomas, A. & Radke, A. K. Increased Responding for Alcohol and Resistance to Aversion in Female Mice. *Alcohol Clin Exp Res* **44**, 1400-1409 (2020). https://doi.org/10.1111/acer.14384
66 Guinle, M. I. B. & Sinha, R. The Role of Stress, Trauma, and Negative Affect in Alcohol Misuse and Alcohol Use Disorder in Women. *Alcohol Res* **40**, 05 (2020). https://doi.org/10.35946/arcr.v40.2.05
67 Borrow, A. P. & Handa, R. J. Estrogen Receptors Modulation of Anxiety-Like Behavior. *Vitamins and hormones* **103**, 27-52 (2017). https://doi.org/10.1016/bs.vh.2016.08.004
68 Zuloaga, D. G., Heck, A. L., De Guzman, R. M. & Handa, R. J. Roles for androgens in mediating the sex differences of neuroendocrine and behavioral stress responses. *Biol Sex Differ* **11**, 44 (2020). https://doi.org/10.1186/s13293-020-00319-2
69 Ryherd, G. L., Bunce, A. L., Edwards, H. A., Baumgartner, N. E. & Lucas, E. K. Sex differences in avoidance behavior and cued threat memory dynamics in mice: Interactions between estrous cycle and genetic background. *Horm Behav* **156**, 105439 (2023). https://doi.org/10.1016/j.yhbeh.2023.105439
70 Miller, C. K. & Meitzen, J. No detectable changes in anxiety-related and locomotor behaviors in adult ovariectomized female rats exposed to estradiol, the ERβ agonist DPN or the ERα agonist PPT. *Horm Behav* **152**, 105363 (2023). https://doi.org/10.1016/j.yhbeh.2023.105363
71 Avery, S. N., Clauss, J. A. & Blackford, J. U. The Human BNST: Functional Role in Anxiety and Addiction. *Neuropsychopharmacology* **41**, 126-141 (2016). https://doi.org/10.1038/npp.2015.185
72 Lebow, M. A. & Chen, A. Overshadowed by the amygdala: the bed nucleus of the stria terminalis emerges as key to psychiatric disorders. *Molecular psychiatry* **21**, 450-463 (2016). https://doi.org/10.1038/mp.2016.1
73 Pleil, K. E. *et al.* NPY signaling inhibits extended amygdala CRF neurons to suppress binge alcohol drinking. *Nat Neurosci* **18**, 545-552 (2015). https://doi.org/10.1038/nn.3972

74 Kuun-Hadden, T., Brar, R., Klemens, M. N., MacLusky, N. J. & Choleris, E. Membrane receptors mediate the rapid facilitation of short-term memory by estradiol in the dorsal hippocampus of female mice. *J Neuroendocrinol* **35**, e13282 (2023). https://doi.org/10.1111/jne.13282
75 Smejkalova, T. & Woolley, C. S. Estradiol acutely potentiates hippocampal excitatory synaptic transmission through a presynaptic mechanism. *J Neurosci* **30**, 16137-16148 (2010). https://doi.org/10.1523/JNEUROSCI.4161-10.2010
76 Oberlander, J. G. & Woolley, C. S. 17beta-Estradiol Acutely Potentiates Glutamatergic Synaptic Transmission in the Hippocampus through Distinct Mechanisms in Males and Females. *The Journal of neuroscience : the official journal of the Society for Neuroscience* **36**, 2677-2690 (2016). https://doi.org/10.1523/JNEUROSCI.4437-15.2016
77 Welch, J. D. *et al.* Single-Cell Multi-omic Integration Compares and Contrasts Features of Brain Cell Identity. *Cell* **177**, 1873-1887.e1817 (2019). https://doi.org/10.1016/j.cell.2019.05.006
78 Hirko, K. A., Spiegelman, D., Willett, W. C., Hankinson, S. E. & Eliassen, A. H. Alcohol consumption in relation to plasma sex hormones, prolactin, and sex hormone-binding globulin in premenopausal women. *Cancer Epidemiol Biomarkers Prev* **23**, 2943-2953 (2014). https://doi.org/10.1158/1055-9965.EPI-14-0982
79 Carroll, H. A., Lustyk, M. K. & Larimer, M. E. The relationship between alcohol consumption and menstrual cycle: a review of the literature. *Arch Womens Ment Health* **18**, 773-781 (2015). https://doi.org/10.1007/s00737-015-0568-2
80 Dozier, B. L. *et al.* Chronic ethanol drinking increases during the luteal menstrual cycle phase in rhesus monkeys: implication of progesterone and related neurosteroids. *Psychopharmacology (Berl)* **236**, 1817-1828 (2019). https://doi.org/10.1007/s00213-019-5168-9
81 Becker, J. & Cha, J. Estrous cycle-dependent variation in amphetamine-induced behaviors and striatal dopamine release assessed with microdialysis. *Behavioural brain research* **35** (1989).
82 Smith, M. A. *et al.* Modulation of heroin intake by ovarian hormones in gonadectomized and intact female rats. *Psychopharmacology (Berl)* **238**, 969-978 (2021). https://doi.org/10.1007/s00213-020-05743-1
83 Sneddon, E. A. *et al.* Gonadal hormones and sex chromosome complement differentially contribute to ethanol intake, preference, and relapse-like behaviour in four core genotypes mice. *Addict Biol* **27**, e13222 (2022). https://doi.org/10.1111/adb.13222
84 Radke, A. K., Sneddon, E. A., Frasier, R. M. & Hopf, F. W. Recent Perspectives on Sex Differences in Compulsion-Like and Binge Alcohol Drinking. *Int J Mol Sci* **22** (2021). https://doi.org/10.3390/ijms22073788
85 Finn, D. A. The Endocrine System and Alcohol Drinking in Females. *Alcohol Res* **40**, 02 (2020). https://doi.org/10.35946/arcr.v40.2.02
86 Sneddon, E. A., Masters, B. M., Shi, H. & Radke, A. K. Removal of the ovaries suppresses ethanol drinking and promotes aversion-resistance in C57BL/6J female mice. *Psychopharmacology (Berl)* **240**, 2607-2616 (2023). https://doi.org/10.1007/s00213-023-06456-x
87 Laredo, S. A., Villalon Landeros, R. & Trainor, B. C. Rapid effects of estrogens on behavior: environmental modulation and molecular mechanisms. *Front Neuroendocrinol* **35**, 447-458 (2014). https://doi.org/10.1016/j.yfrne.2014.03.005
88 Wnuk, A., Przepiórska, K., Pietrzak, B. A. & Kajta, M. Emerging Evidence on Membrane Estrogen Receptors as Novel Therapeutic Targets for Central Nervous System Pathologies. *Int J Mol Sci* **24** (2023). https://doi.org/10.3390/ijms24044043
89 Srivastava, D. P., Woolfrey, K. M. & Penzes, P. Insights into rapid modulation of neuroplasticity by brain estrogens. *Pharmacol Rev* **65**, 1318-1350 (2013). https://doi.org/10.1124/pr.111.005272
90 Abrahám, I. M., Todman, M. G., Korach, K. S. & Herbison, A. E. Critical in vivo roles for classical estrogen receptors in rapid estrogen actions on intracellular signaling in mouse brain. *Endocrinology* **145**, 3055-3061 (2004). https://doi.org/10.1210/en.2003-1676

91 Jain, A. & Woolley, C. S. Mechanisms That Underlie Expression of Estradiol-Induced Excitatory Synaptic Potentiation in the Hippocampus Differ between Males and Females. *J Neurosci* **43**, 1298-1309 (2023). https://doi.org/10.1523/JNEUROSCI.2080-19.2023

92 Stincic, T. L., Grachev, P., Bosch, M. A., Rønnekleiv, O. K. & Kelly, M. J. Estradiol Drives the Anorexigenic Activity of Proopiomelanocortin Neurons in Female Mice. *eNeuro* **5** (2018). https://doi.org/10.1523/ENEURO.0103-18.2018

93 Martinez, L. A. *et al.* Estradiol Facilitation of Cocaine Self-Administration in Female Rats Requires Activation of mGluR5. *eNeuro* **3** (2016). https://doi.org/10.1523/ENEURO.0140-16.2016

94 Krashes, M. J. *et al.* An excitatory paraventricular nucleus to AgRP neuron circuit that drives hunger. *Nature* **507**, 238-242 (2014). https://doi.org/10.1038/nature12956

95 McLean, A. C., Valenzuela, N., Fai, S. & Bennett, S. A. Performing vaginal lavage, crystal violet staining, and vaginal cytological evaluation for mouse estrous cycle staging identification. *J Vis Exp*, e4389 (2012). https://doi.org/10.3791/4389

96 Blue, S. W. *et al.* Simultaneous quantitation of multiple contraceptive hormones in human serum by LC-MS/MS. *Contraception* **97**, 363-369 (2018). https://doi.org/10.1016/j.contraception.2018.01.015

97 Administration, U. S. F. a. D. (2018).

98 Team, R. C. (R Foundation for Statistical Computing, Vienna, Austria, 2021).

99 Hao, Y. *et al.* Integrated analysis of multimodal single-cell data. *Cell* **184**, 3573-3587.e3529 (2021). https://doi.org/10.1016/j.cell.2021.04.048

100 Thiele, T. E. & Navarro, M. "Drinking in the dark" (DID) procedures: a model of binge-like ethanol drinking in non-dependent mice. *Alcohol* **48**, 235-241 (2014). https://doi.org/10.1016/j.alcohol.2013.08.005

Funding
This research was supported by: NIH grants K99/R00 AA023559 and R01 AA027645, a NARSAD Young Investigator Award, a Stephen and Anna-Maria Kellen Foundation Junior Faculty Award 26608 (K.E.P.); NIH grant F31 AA029293 (L.J.Z.); NIH grant T32 DA039080 (J.K.R.I., L.J.Z., O.B.L.). C.K.H. was supported by a Medical Scientist Training Program grant from the National Institute of General Medical Sciences of the National Institutes of Health under award number: T32GM007739 to the Weill Cornell/Rockefeller/Sloan Kettering Tri-Institutional MD-PhD Program. P.B. was supported by a Deutsche Forschungsgemeinschaft (DFG) Walter Benjamin Fellowship (516215326). The Endocrine Technologies Core (ETC) at Oregon National Primate Research Center (ONPRC) is supported (in part) by NIH grant P51 OD011092 for operation of the Oregon National Primate Research Center.